JOURNAL OF SOLID STATE CHEMISTRY 2, 68–73 (1970)

Crystal Chemistry and Properties of Phases in the System SrO-PbO-O

KENNETH L. KEESTER* AND WILLIAM B. WHITE†

Materials Research Laboratory, The Pennsylvania State University,
University Park, Pennsylvania 16802

Received October 31, 1969

The system SrO–PbO_2 is shown to contain two compounds, $SrPbO_3$ and Sr_2PbO_4. $SrPbO_3$ is an orthorhombic distortion of the perovskite structure. Sr_2PbO_4 is considered the type example of a newly described structure type. Precise unit cell and powder data are presented for these phases. High temperature diffractometry shows a transition from orthorhombic to tetragonal $SrPbO_3$ at 450°C. This transition is not reflected in the dielectric constant. IR spectra for the compounds are presented.

Introduction

Tetravalent lead oxides of calcium and barium are well known and are important industrial materials. Ba_2PbO_4 has the K_2NiF_4 structure and $BaPbO_3$ is a cubic perovskite. Ca_2PbO_4, long thought to be hexagonal, has recently been shown to be a member of a new structure type (*1*). $CaPbO_3$ has an unknown structure. Since Ca^{++} and Ba^{++} plumbates have a different crystal chemistry, it is of interest to examine the behavior of the Sr^{++} ion which is of intermediate size.

Compounds in the system also provide an opportunity to examine the vibrational frequencies of the Pb^{4+} ion. The high charge would normally imply a fairly high vibrational frequency while the high mass would tend to lower the frequency.

Experimental Methods

Initially the system was investigated with high-oxygen pressure techniques. No new oxides were found that required stabilization by high oxygen pressure. The oxides found were $SrPbO_3$ and Sr_2PbO_4, both of which can be prepared at atmospheric pressure if special techniques are used. Mechanical mixtures of oxides do not yield pure phase materials. At low temperatures, reactions do not proceed while at high temperatures the volatility of lead oxide becomes appreciable before reactions are complete.

Bulk quantities of pure phase $SrPbO_3$ and Sr_2PbO_4 were prepared by the following method. Stoichiometric mixtures of PbO_2 and $Sr(OH)_2 \cdot 8H_2O$ were weighed out and ground repeatedly under acetone until finely homogeneous powders were obtained. The SrO equivalent of the hydroxide was predetermined by thermogravimetric analysis to account for its varying water content.

Pure phase Sr_2PbO_4 was prepared from finely powdered starting material thinly dispersed on gold sheet. The same material pelletized or used as piles of powder will sinter to products containing SrO on the surface and $SrPbO_3$ in the interior. The surface area must be large with respect to reactant volume to suppress diffusion or transport of SrO.

Conversely, for preparation of pure $SrPbO_3$, the reactant volume must be large with respect to surface area. Sr_2PbO_4 forms on the surface of mixtures of $SrPbO_3$ stoichiometry. Sintered disks from predensified $SrPbO_3$ can be prepared by burying them in additional powdered $SrPbO_3$ before sintering.

Crystallographic Characterization of Phases

One might expect a K_2NiF_4 structure common to Ba_2PbO_4, for the strontium compound; however, Sr_2PbO_4 has a unique and new structure type. The structure, reported by Trömel (*1*) shows the large cation in sevenfold coordination and the small cation in sixfold coordination. The structure is referred to as the Sr_2PbO_4 structure type.

X-ray powder diffraction data for Sr_2PbO_4 are given in Table I. Material used to measure powder data was prepared in the manner described above;

---

* Present address, IBM Research Division, Building 025, Monterey and Cottle Roads, San Jose, California 95114.

† Also affiliated with the Department of Geochemistry and Mineralogy.

TABLE I

X-RAY POWDER DIFFRACTION DATA FOR Sr_2PbO_4

Orthorhombic $2/m\ 2/m\ 2/m$ Sp.G. *Pbam* or *Pba*2
$a_0 = 6.162 \pm 0.001$ Å
$b_0 = 10.079 \pm 0.001$ Å
$c_0 = 3.505 \pm 0.001$ Å
$Z = 2$
$D_x = 6.810$ g/cm^3 I/I_1 = relative peak height

h k l	*d* Å (calcd)	*d* Å (meas)	I/I_1
1 1 0	5.2575	5.26	36
0 2 0	5.0396	5.04	6
1 2 0	3.9011	3.90	5
2 0 0	3.0811	3.08	31
1 3 0	2.9498	2.95	92
1 1 1	2.9162	2.91_7	100
0 2 1	2.8773	2.87_9	46
2 2 0	2.6288	2.63_0	7
1 2 1	2.6071	2.61_1	2
0 4 0	2.5198	2.52_1	9
1 4 0	2.3323	2.33_2	10
2 0 1	2.3140	2.315	7
2 1 1	2.2554	2.255_2	20
2 2 1	2.1029	2.103_4	55
0 4 1	2.0459	2.045_9	14
3 1 0	2.0127	2.012_3	9
2 4 0	1.9506	1.950_6	8
1 5 0	1.9159	1.915_1	2
3 2 0	1.9022	1.902_3	7
3 3 0	1.7525	1.752_1	27
3 1 1	1.7454	1.746_8	23
2 4 1	1.7044	1.7045	17
1 5 1	1.6811	1.6808	46
3 2 1	1.6718	1.6726	9
1 1 2	1.6624	1.6623	7
3 4 0	1.5921	1.5923	4
3 3 1	1.5675	1.5677	9
4 0 0	1.5406	1.5408	1
4 1 0	1.5229	1.5231	10
1 3 2	1.5066	1.5067	23
4 2 0	1.4733	1.4740	12
2 2 2	1.4581	1.4581	2
3 4 1	1.4496	1.4499	3
3 5 0	1.4387	1.4390	5
4 0 1	1.4103	1.4105	4
1 4 2	1.4009	1.4009	4
4 1 1	1.3967	1.3973	5
4 2 1	1.3581	1.3586	5
3 5 1	1.3310	1.3310	5
3 1 2	1.3216	1.3217	4
4 4 0	1.3145	1.3146	4
1 7 1	1.3018	1.3021	6*b*
3 2 2	1.2888	1.2889	3
3 3 2	1.2392	1.2391	5
4 4 1	1.2307	1.2308	3
5 1 0	1.2233	1.2232	5
0 6 2	1.2127	1.2127	5
0 8 1	1.1856	1.1858	4
3 4 2	1.1784	1.1788	3
5 1 1	1.1550	1.1553	2
4 1 2	1.1495	1.1495	1
1 1 3	1.1404	1.1403	5
2 6 2	1.1284	1.1283	8
3 7 1	1.1175	1.1177	2
3 5 2	1.1120	1.1121	2
2 8 1	1.1065	1.1067	5
1 9 0	1.1019	1.1022	3
5 3 1	1.0987	1.0988	7
1 7 2	1.0948	1.095_5	4*b*

temperature 927°C, duration 22 hr. The diffraction specimen was prepared by grinding sintered Sr_2PbO_4 to a fine powder under CCl_4 and then smear-mounting on a glass slide. Data were collected on a Siemans diffractometer using alpha quartz as an internal standard.

Refined cell constants and standard error for Sr_2PbO_4 as derived in this manner are tabulated below. Data from the single-crystal structure analysis are given for comparison.

	This Work	Trömel (*1*)
a	6.162 Å ± 0.001 Å	6.15_5 Å
b	10.079 Å ± 0.001 Å	10.0_6 Å
c	3.505 Å ± 0.001 Å	3.49_8 Å

Indexed reflections were consistent with extinction conditions for *Pbam* (or the acentric, *Pba*2) and the complete calculated pattern contains these conditions.

Using 1.6602 for a combined Avogadro number and units-conversion factor with ^{12}C atomic weights (International Union of Pure and Applied Chemistry, 1961) the calculated X-ray density for Sr_2PbO_4 at 25°C is 6.810 g/cm^3 from cell volume of 217.69 ± 0.04 Å^3.

Axial ratios are

$$A = \frac{a}{b} = 0.6114 \text{ and } C = \frac{c}{b} = 0.3477.$$

Absolute intensity of the pattern was measured according to Hanawalt (*2*). The strongest line of Sr_2PbO_4 and Linde A type Al_2O_3 in a 50:50 weight percent mechanical mixture of these components was slow-scanned and recorded. The intensity ratio of the diffracting power of Sr_2PbO_4 to α-Al_2O_3 is 3.0_0.

$SrPbO_3$ was first reported by Weiss (*3*). Its symmetry has been described as an orthorhombic distortion of the perovskite structure. While Weiss did report an indexed powder pattern from Debye–Scherrer data, no intensities were given for any of the reflections.

Material used to measure X-ray diffraction powder data was not prepared in the manner described in a previous section. Reaction conditions were 500°C, with 2015-bar oxygen pressure for a duration of 72 hr. The material appears identical to atmospheric preparations.

Specimen preparation, pattern production, and alpha-quartz standardization were carried out by procedures identical to those used for Sr_2PbO_4. The pattern exhibits a pronounced pseudocubic appearance. The strongest lines or line groups can be indexed on a simple cubic perovskite cell. At low 2θ angles, the deviation from a cubic pattern is not pronounced due to lack of resolution of equivalent reflections especially if patterns are made with poorly crystalline material. All other *noncubic* reflections are very weak. At high 2θ angles splitting of *cubic* reflections becomes apparent.

The low angle portion of our pattern was initially indexed with a pattern calculated from Weiss' cell constants and Smith's (*4*) program. Then the data were refined with the least-squares program. Refined cell constants and standard error are tabulated below with previously reported cell constants.

	This work	Weiss (3)
a	5.860 ± 0.001 Å	5.864 ± 0.005 Å
b	5.958 ± 0.001 Å	5.959 ± 0.005 Å
c	8.331 ± 0.001 Å	8.336 ± 0.005 Å

Complete X-ray powder diffraction data for the forward reflection region are compiled in Table II. This pattern (and cell constants derived from it) should be superior to Weiss' data for reasons following. Conventionally, Debye–Scherrer film strips are only read to $\pm 0.05^\circ$ 2θ or at best $0.02_5{}^\circ$ 2θ. With the described diffractometer techniques, patterns can be measured to $\pm 0.01^\circ$ 2θ. Weiss reports data only to 63° 2θ while Table II includes all reflections up to 90° 2θ. In addition, cell constants are based on a refinement of 54 reflections (including α_2 reflections) compared to 28 reported by Weiss.

All reflections are consistent with space groups *Pnma* or $Pna2_1$. The former is centric, the latter is a piezoelectric and pyroelectric, acentric space group. The two space groups are indistinguishable by X-ray (powder) methods. The complete pattern was calculated with conditions, $0kl: k + l = 2n$ and $hk0: h = 2n$ (*5*).

TABLE II

X-RAY POWDER DIFFRACTION DATA FOR $SrPbO_3$

Orthorhombic Sp.G. *Pnma* or $Pna2_1$
$a_0 = 5.860 \pm 0.001$Å
$b_0 = 5.958 \pm 0.001$Å
$c_0 = 8.331 \pm 0.001$Å
$D_x = 7.827$ g/cm^3 I/I_1 = relative peak height

h k l	*d* Å (calcd)	*d* Å (meas)	I/I_1
0 0 2	4.125	4.17_7	24
1 1 1	3.735	3.73_8	3
0 2 0	2.979	2.980	33
1 1 2	2.950	2.951	100
2 0 0	2.930	2.932	24
1 0 3	2.509	2.511	2
0 2 2	2.423	2.426	5
2 0 2	2.397	2.399	4
1 1 3	2.313	2.313	2
2 2 0	2.089	2.089	33
0 0 4	2.083	2.054	3
2 2 1	2.026	2.029	3
1 1 4	1.864	1.865	19
1 3 1	1.835	1.835	3
1 3 2	1.714	1.715	26
0 2 4	1.707	1.707	22
3 1 2	1.695	1.697	40
1 3 3	1.5574	1.557_5	1
0 4 0	1.4896	1.4899	3
2 2 4	1.4749	1.4748	18
4 0 0	1.4651	1.4651	5
0 4 2	1.4026	1.4028	3
1 3 4	1.3959	1.3961	5
3 1 4	1.3857	1.3858	4
2 4 0	1.3278	1.3281	5
3 3 2	1.3208	1.3208	12
1 1 6	1.3176	1.3174	18
2 4 2	1.2651	1.2653	3
0 2 6	1.2585	1.2581	2
4 2 2	1.2537	1.2541	4
0 4 4	1.2116	1.2117	5
4 0 4	1.1983	1.1983	5
4 3 1	1.1674	1.1680	2
1 5 1	1.1565	1.1568	4
1 5 2	1.1244	1.1244	4
2 4 4	1.1196	1.1186	4
1 3 6	1.1171	1.1166	8
4 2 4	1.1117	1.1116	14
5 1 2	1.1086	1.1086	13

Using 1.6602 for a combined Avogadro number and units-conversion factor and ^{12}C atomic weights the calculated X-ray density of $SrPbO_3$ at 25°C is 7.827 g/cm^3. Weiss (*3*) reports a measured density of 7.76 g/cm^3, in good comparison considering

difficulty involved in measuring densities on powders or sintered ceramics. Error due to adsorbed gas on particles or pore space in ceramics will lower density. The cell contains four perovskite formula units, and has a volume of 290.89 ± 0.13 Å^3.

Axial ratios are:

$$A = \frac{a}{b} = 0.9836 \text{ and } C = \frac{c}{b} = 1.398.$$

Absolute intensity of the pattern, measured according to Hanawalt (*2*) and described above, is 5.1_9.

Phase Transitions in SrPbO$_3$

Numerous ABO$_3$-type compounds having an orthorhombically distorted perovskite structure are known and have been studied, principally for their dielectric properties. Some perovskites show a sequence of phase transitions. From low to high temperature the sequence is hexagonal (rhombohedral) to orthorhombic, tetragonal, and finally cubic. The orthorhombic cell can also be indexed on a monoclinic pseudocell and is useful in showing the sheared relationship to the cubic cell. Because orthorhombic ABO$_3$ perovskites can have a high temperature ferroelectric phase, an investigation of SrPbO$_3$ was appealing. Black SrPbO$_3$ is nontransparent in the optical region of the spectrum, so hot-stage optical microscopy was not possible.

The method of investigation was high-temperature X-ray diffractometry, using a Tem-Pres X-ray Diffraction Furnace mounted on a Picker diffractometer. With this equipment change in the unit cell size as well as the change in symmetry can be measured as a function of temperature.

The diffractometer specimen consisted of SrPbO$_3$ powder mixed with an adequate amount of α-quartz calibrant. Internal standardization was deemed necessary to correct for thermal expansion-induced errors in experimental assembly. Alpha-quartz was selected because the coefficients of thermal expansion are well known and because several fairly strong lines bracket the desired reflections to be observed.

Change in cell size with temperature and the orthorhombic-to-tetragonal transformation was observed by monitoring orthorhombic {132}, {024}, and {312} reflections of the SrPbO$_3$ powder pattern at intervals of increasing temperature. These reflections were chosen for reasons of intensity and ease of calculation. Strong lines are needed because the intensities decrease due to line broadening at high temperatures. Cell constants can be calculated from these three reflections by simultaneous solution. Patterns were made by slowly scanning (1/4° 2θ/min) a region from 50–60° 2θ which contains the three reflections bracketed by α-quartz standard lines. Resolution was sufficient to measure to 0.01° 2θ. Thermal expansion data for α-quartz came from Jay (*6*) and was used to calculate standard peak positions at various temperatures.

TABLE III

TRANSFORMATION OF MILLER INDICES FOR SrPbO$_3$

(The cubic and {204} of the orthorhombic cell were not observed. The second setting was used for the monoclinic cell. Brackets enclose equivalent planes.)

Monoclinic		Orthorhombic		Tetragonal		Cubic
$\{\bar{2}11\}$	=	{132}	→	211 121	→	211 121 112
$\{\bar{1}21\}$	=	{024}	→			
{121}	=	{204}				
{211}	=	{312}	→	{112}	→	

At about 450°C the {132} and {024} reflections merge and transform into {211} of the tetragonal cell. The {312} reflection remains unchanged in position but now constitutes the tetragonal {112}. Table III shows the transformation of these planes with ascent of symmetry.

Measurements were made up to 573°C, the temperature of the α-to-β transition in the quartz standard. Figure 1 is a plot of the cell constants versus temperature. At about 450°C orthorhombic SrPbO$_3$ changes to a tetragonal form via a first-order phase transition evidence by volume discontinuity at the transition temperature. Slight volume contraction on transformation from orthorhombic to tetragonal is not unexpected and has been observed

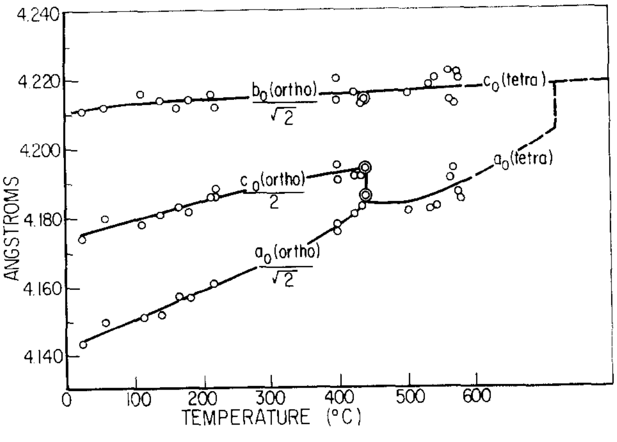

FIG. 1. Plot of SrPbO$_3$ cell constants versus temperature.

in $BaTiO_3$ by Kay and Vousden (7). Above 550°C the specimen is rapidly attacked by air, and Sr_2PbO_4 forms on the diffraction surface. The expected first-order phase transition to a cubic form could not be observed.

Dielectric Properties of $SrPbO_3$

Material used to prepare dielectric wafers was initially prepared by sintering a stoichiometric powder of strontium hydroxide hydrate and lead dioxide. The powder was prepared by repeated grinding of the reagents under acetone to insure uniformity. Sintering took 24 hr at 900°C inside a gold foil-lined ceramic crucible. Only interior portions of vesicular lump material were $SrPbO_3$, exterior portions being Sr_2PbO_4 where reaction took place in contact with air. Pure pieces of $SrPbO_3$ were then selected from the crushed lump and reground with a slight addition of starting material to serve as a binder. After pressing this powder, the resultant wafer was buried in a crucible of starting material and resintered at 940°C for 15 hr. This technique produces a high-density ceramic wafer of good mechanical strength. The wafer was then polished to a thickness of 0.28 mm and evaporated gold contacts were placed on each side with additional gold epoxy baked on evaporated areas to insure good contacts.

Capacitance and conductivity measurements were made as a function of temperature with the sample heated inside a resistance wound tube furnace. Temperature was measured with a chromel-alumel thermocouple and potentiometer with ice bath standard junction. The wafer was placed on a platinum stage that served as one contact, the other probe contact was drawn down on the specimen by gravity. Capacitance and conductivity readings were taken with a Wayne Kerr Model B201 bridge operating at 1 Mc/s.

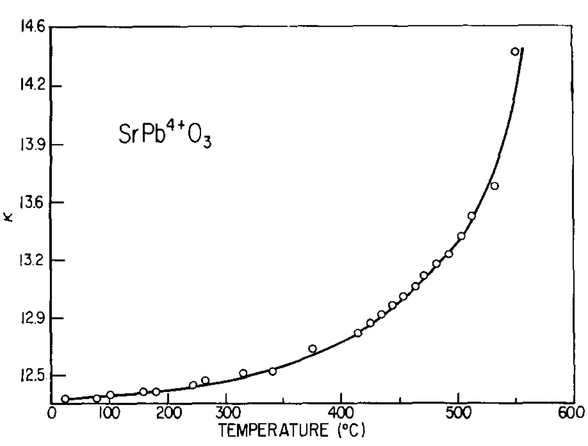

FIG. 2. Dielectric constant versus temperature for ceramic $SrPbO_3$.

The dielectric constant is plotted as a function of temperature in Fig. 2. The curve shown is reproducible on the heating cycle but above 550° the conductivity rises rapidly and no meaningful measurements can be made. This is due to reaction of the $SrPbO_3$ surface with air forming Sr_2PbO_4. This surface reaction proceeds rapidly above 550°C.

There is no apparent change in dielectric response at the 450°C orthorhombic-to-tetragonal transition. The rapid rise in the curve in the vicinity of 550°C apparently indicates Maxwell–Wagner dielectric phenomena from the magnitude of the permittivity and correlates with a rapid rise in $\tan\delta$.

Infrared Spectra

Infrared spectra on these materials were measured in CsI pellets using a Perkin-Elmer model 621 spectrophotometer. Powdered oxides were mixed with 1000 mg of CsI, and cold-pressed under vacuum with an annealing of three cycles of 5-min pressure followed by 5 min with no pressure. This technique gave the maximum clarity of the specimen disks.

Sr_2PbO_4 is the type compound for a structural family whose members include Cd_2PbO_4, Ca_2PbO_4, Cd_2SnO_4, Ca_2SnO_4, and the high pressure form of Mn_2GeO_4. Therefore, a factor group analysis applies as well to these compounds. The space group is *Pbam*, D_{2h}^9, with two Sr_2PbO_4 per unit cell. The site occupations of the ions are:

Ion	Equipoint	Symmetry
Sr^{++}	4(*h*)	C_s
Pb^{4+}	2(*a*)	C_{2h}
O^{2-}	4(*h*)	C_s
O^{2-}	4(*g*)	C_s

This leads to the invariance conditions given in Table IV and the normal modes and selection rules shown in Table V.

$SrPbO_3$, although orthorhombically distorted, gives an infrared spectrum very similar to those known for undistorted perovskites. Because little additional factor-group splitting was observed, a factor-group analysis was not performed. Analysis of the cubic perovskite structure (8) gives three T_{1u} ir-active modes and one T_{1u} acoustic mode.

The infrared spectrum of Sr_2PbO_4 is shown in Fig. 3. Only five to six of the predicted 17 infrared active vibrations are observed in the measured frequency range. Both overlap of close-lying bands

TABLE IV

INVARIANCE CONDITIONS FOR Sr_2PbO_4

D_{2h}	E	$C_2(z)$	$C_2(y)$	$C_2(x)$	i	$\sigma(xy)$	$\sigma(xz)$	$\sigma(yz)$
C_s	E	–	–	–	–	σ_h	–	–
4Sr	4	0	0	0	0	4	0	0
C_{2h}	E	C_2	–	–	i	σ_h	0	0
2Pb	2	2	0	0	2	2	0	0
C_s	E	–	–	–	–	σ_h	–	–
$4\,0_1$	4	0	0	0	0	4	0	0
C_s	E	–	–	–	–	σ_h	–	–
$4\,O_2$	4	0	0	0	0	4	0	0
Total ω_r	14	2	0	0	2	14	0	0
$\chi(R)$	42	−2	0	0	−6	14	0	0

TABLE V

NORMAL MODES AND SELECTION RULES FOR Sr_2PbO_4

D_{2h}	Total Modes	Acoustic	Vibrations	Selection Rules
A_g	6	—	6	Raman
B_{1g}	6	—	6	Raman
B_{2g}	3	—	3	Raman
B_{3g}	3	—	3	Raman
A_u	4	—	4	—
B_{1u}	4	z	3	ir, $E\|c$
B_{2u}	8	y	7	ir, $E\|b$
B_{3u}	8	x	7	ir, $E\|a$

and the occurrence of bands at still lower frequencies may be responsible. Of greatest interest is the 551 cm^{-1} high-frequency band. It is very sharp, which usually indicates a high degree of covalent bonding.

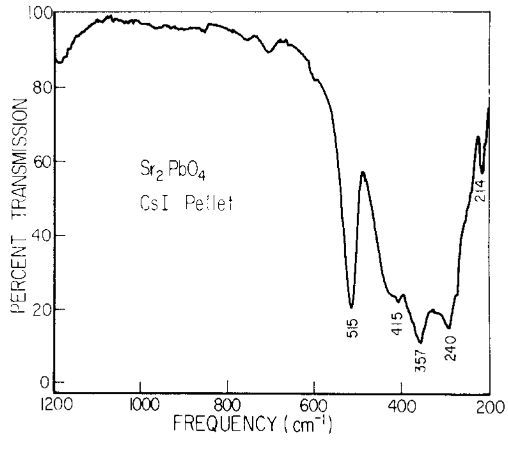

FIG. 3. Infrared spectrum of powdered Sr_2PbO_4.

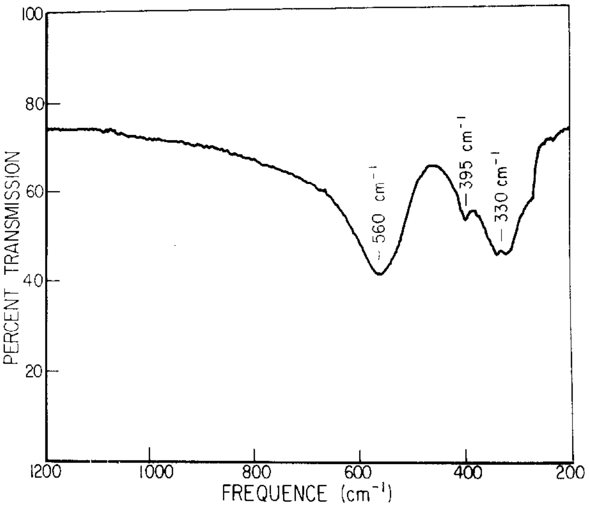

FIG. 4. Infrared spectrum of powdered $SrPbO_3$, orthorhombic perovskite.

The absorption cutoff is low and there is a sharp boundary between the ir-transmitting region above 700 cm^{-1} and the absorption region.

The spectrum of $SrPbO_3$ (Fig. 4) shows three infrared bands as predicted by the theoretical analysis of the ideal cubic perovskite structure. The assignments [according to Hunt et al. (*8*)] would be $\nu_1 = 560$ cm^{-1}, Pb–O stretch, $\nu_2 = 395$ cm^{-1}, Pb–O–Pb bend, and $\nu_3 = 330$ cm^{-1}, the Sr–PbO_3 stretch. These compare well with the spectra of other perovskites reported by Last (*9*).

Acknowledgments

This research was supported in part under Contract N00014-67-A-0385-0005, a part of Project Defender, jointly sponsored by the Advanced Research Projects Agency, The Office of Naval Research, and the Department of Defense. We are grateful to Professor L. E. Cross for the loan of the dielectric measurement equipment.

References

1. M. TRÖMEL, *Naturwiss.* **52**, 492 (1965).
2. J. D. HANAWALT, personal communication, 1968.
3. R. WEISS, *C.R. Acad. Sci. Paris* **246**, 3073 (1958).
4. D. K. SMITH, Lawrence Radiation Laboratory Report UCRL 50264, Livermore, California, 1967.
5. K. L. KEESTER, "Crystal Chemistry, Phase Equilibria, and Properties of Ternary Lead-Oxygen Systems," Ph.D. Thesis, The Pennsylvania State University, 1969.
6. A. H. JAY, *Proc. Roy. Soc. London* **142**, 237 (1933).
7. H. F. KAY AND P. VOUSDEN, *Phil. Mag.* **40**, 1019 (1949).
8. G. R. HUNT, C. H. PERRY, AND J. FERGUSON, *Phys. Rev.* **134**, A688 (1964).
9. J. T. LAST, *Phys. Rev.* **105**, 1740 (1957).